RSC Advances

PAPER

View Article Online
View Journal | View Issue

Cite this: *RSC Adv.*, 2025, **15**, 13574

Effects of gamma radiation on the properties of GO/PVA/AgNW nanocomposites

Mustafa Muradov,[a] Elchin Huseynov,[b] Marjetka Conradi,[c] Matjaz Malok,[d] Tina Sever[c] and Mahammad Baghir Baghirov[*a]

In this study, GO/PVA/AgNWs nanocomposites were exposed to gamma irradiation at doses of 8, 25, and 50 kGy to investigate the effects of gamma radiation on their structural and morphological properties. Structural modifications induced by irradiation were examined using X-ray diffraction (XRD) analysis and Raman spectroscopy, while morphological changes were evaluated through scanning electron microscopy (SEM). The findings demonstrate that gamma irradiation significantly affects the crystallinity of the nanocomposites. Although no considerable morphological alterations were observed, Raman spectroscopy confirmed the presence of radiation-induced structural defects. Analysis of the I_D/I_G ratio revealed that the most prominent defect formation occurred in the sample irradiated with 8 kGy, which exhibited an I_D/I_G ratio of 1.07. Furthermore, the study underscores the influence of gravitational forces during the composite fabrication process, as evidenced by the preferential accumulation of fillers in the lower regions of the nanocomposites. This phenomenon was validated through both XRD and SEM analyses. Overall, the study offers valuable insights into the role of gravitational effects in composite formation and elucidates the influence of low-dose gamma irradiation on the structural integrity, morphology, and optical characteristics of GO/PVA/AgNWs nanocomposites.

Received 24th February 2025
Accepted 23rd April 2025

DOI: 10.1039/d5ra01344e

rsc.li/rsc-advances

1 Introduction

In recent years, polymer nanocomposites have garnered significant interest due to their unique properties and lightweight nature. The versatile characteristics of nanocomposites make them applicable in various fields.[1,2] Polymer nanocomposites are formed by combining polymer matrices with nanofillers such as carbon-based nanoparticles, metal nanoparticles, metal oxide nanoparticles, and others.[3,4] Due to their wide range of applications, polymer nanocomposites have attracted considerable attention from the scientific community, including uses in conductive coatings, sensors, energy storage devices, and more.[5,6] Among these, nanocomposites with PVA (polyvinyl alcohol) matrices stand out prominently. PVA is an excellent polymer matrix for hybrid nanoparticles because of its superior thermal stability, chemical resistance, film-forming ability, high mechanical strength, and water solubility. Notably, PVA effectively prevents the agglomeration of nanoparticles. Cross-linking reactions associated with PVA are widely employed to enhance its physical properties.[7,8] The hydrophilic nature of PVA facilitates the creation of composites with graphene oxide (GO), which is also water-soluble.[9] In GO/PVA-based nanocomposites, GO is uniformly dispersed, enabling the formation of homogeneous composites.[10] Furthermore, when multi-layered GO is used, it can intercalate between polymer layers and create new orientations.[11] Studies have shown that the reduction of GO in GO/PVA composites decreases defects, improves crystallinity, and enhances thermal conductivity.[12] Additionally, the properties of such composites can be tailored by altering the concentration of GO within the polymer matrix. Yashia I. S. *et al.* determined that the absorption coefficient of (PVA/GO) nanocomposites increase with the concentration of GO nanoparticles, while the bandgap decreases. The AC electrical conductivity of (GO/PVA) nanocomposites increases with frequency and the concentration of GO nanoparticles.[13] Due to their tunable properties, these composites hold potential applications in sensors, membranes, supercapacitors, and more.[14–16] However, research on graphene oxide-based nanomaterials has been limited by poor dispersion and processing capabilities. To overcome this, noble metal nanoparticles such as silver (Ag) have been widely utilized with GO to enhance stability and prevent the restacking of GO layers. Researchers have conducted extensive studies on composites of graphene-based materials decorated with Ag nanoparticles, offering various intriguing properties.[17,18] On the other hand, GO sheets can prevent contact between Ag nanowires, thus maintaining the 1D structure of the nanowires.[19] Literature on GO/PVA/Ag ternary composites remains limited. However, R. M. Attia *et al.* investigated the effects of electron beam radiation on such composites.[20]

[a]*Nano Research Laboratory, Baku State University, 23 Academik Zahid Khalilov Street, Baku, AZ1148, Azerbaijan. E-mail: bmbaghir@gmail.com*
[b]*Institute of Radiation Problems of the Ministry of Science and Education of the Republic of Azerbaijan, B. Vahabzade 9, AZ 1143, Baku, Azerbaijan*
[c]*Institute of Metals and Technology, Lepi pot 11, 1000, Ljubljana, Slovenia*
[d]*Jožef Stefan Institute, Jamova cesta 39, Ljubljana 1000, Slovenia*

Another intriguing aspect is the modification of materials using gamma radiation. Research in this area has particularly focused on the effects of ϒ radiation on the properties of carbon materials. Studies reveal that ϒ radiation can alter the oxygen content in such compounds.[21] Atta M. M. *et al.* reported that the maximum specific capacitance of GRGO prepared at 80 kGy increased to ~174 F g^{-1}.[22] Dumée L. F. *et al.* found that the electrical conductivity of reduced GO increased by 400 times under gamma radiation.[23] Literature also demonstrates that ϒ irradiation can induce large and stable hole concentrations in graphene.[24] Studies on GO/PMMA composites suggest their potential application in gamma radiation dosimetry.[25] For GO/PVA composites, ϒ radiation has been shown to play a central role in the reduction of GO and the formation of cross-links.[26] Furthermore, it has been determined that the bandgap decreases when such composites are modified with ϒ radiation.[27,28] In GO/AgNWs composites, strain calculations indicate that the strain reaches a maximum value for GO at a dose of 25 kGy under gamma radiation.[29]

In this study, the structural and morphological changes in samples irradiated with different gamma doses (8, 25, and 50 kGy) were investigated. The primary objective was to explore the physical processes occurring in these composites under the influence of gamma radiation. To achieve this, X-ray diffraction (XRD), scanning electron microscopy (SEM), and Raman spectroscopy analyses were conducted, and the obtained results were thoroughly discussed.

2 Materials and methods

2.1 Synthesis of graphene oxide (GO)

Graphene oxide (GO) was synthesized using a modified Hummers' method.[30,31] To begin, 3 g of graphite powder and 1.5 g of sodium nitrate ($NaNO_3$) were placed in a 500 ml container. Then, 70 ml of concentrated sulfuric acid (H_2SO_4) was added to the mixture, which was subsequently cooled to 0 °C using an ice bath. The mixture was stirred for 1 hour under these conditions with a magnetic stirrer. Gradually, potassium permanganate ($KMnO_4$) was added at a controlled rate, ensuring the reaction temperature remained below 20 °C. After $KMnO_4$ addition, the mixture was stirred for 3 hours, followed by stirring for an additional hour at 35 °C after removing it from the ice bath. Next, 150 ml of water was slowly added while maintaining stirring at 98 °C for 30 minutes. Subsequently, 300 ml of water was gradually added, and the mixture was stirred for an additional hour. To conclude the reaction, 15 ml of 30% hydrogen peroxide (H_2O_2) was introduced, and the mixture was stirred for 30 minutes. The resulting product was filtered through filter paper and washed with 250 ml of distilled water containing hydrochloric acid (HCl) in a 1 : 10 ratio to remove residual metal ions. Finally, the GO product was dried at room temperature.

2.2 Synthesis of silver nanowires (AgNWs)

Silver nanowires (AgNWs) were synthesized following a modified polyol method inspired by prior research.[32,33] Ethylene glycol (EG) was utilized as both a solvent and a reducing agent, while polyvinylpyrrolidone (PVP, molecular weight: 360 000) served as a stabilizing capping agent. Sodium chloride (NaCl) and $CuBr_2$ were employed to maintain charge balance and support nanowire growth. The process began by dissolving PVP in EG at a concentration of 295.6 mM, which was stirred for 3 hours at an elevated temperature and then cooled to room temperature. Separate solutions of $CuBr_2$ (3.2 mM) and NaCl (15.7 mM) in EG were prepared for later use. Silver nitrate ($AgNO_3$) was dissolved in EG to achieve a concentration of 187.8 mM. For the synthesis, 5 ml of EG was placed in a 20 ml vial and heated in a silicone oil bath at 160 °C. After 10 minutes, 100 μl of $CuBr_2$ and 150 μl of NaCl solutions were injected into the vial. Subsequently, 1.5 ml of $AgNO_3$ and 1.5 ml of PVP solutions were added dropwise over a 15-minute period. The reaction was maintained for 1.5 hours before cooling to room temperature. To collect the silver nanowires, acetone was added to the reaction mixture to precipitate the product. The precipitates were isolated by centrifugation at 4000 rpm for 8 minutes and washed three times with acetone to remove residual chemicals. The final product was dispersed in ethanol for further use.

2.3 Preparation of GO/PVA/AgNWs nanocomposites

As illustrated in Fig. 1, the fabrication of GO/PVA/AgNWs nanocomposites involved a multi-step solution-casting process designed to ensure uniform dispersion and optimal interaction among the composite components. Initially, PVA of medium molecular weight was dissolved in distilled water (DW) at elevated temperature (~60 °C) until a clear, homogeneous solution was obtained. In a separate beaker, GO was also dispersed in distilled water and sonicated for several minutes to promote exfoliation and uniform suspension of GO sheets. Once both solutions were prepared, the GO suspension was gradually added to the PVA solution under vigorous stirring to prevent aggregation. The resulting mixture was subjected to ultrasonic treatment for 6 minutes using a probe-type ultrasonicator. This step was critical for enhancing the interfacial interaction between the GO sheets and the PVA polymer chains.

Following the initial sonication, a predetermined amount of AgNWs was introduced into the GO/PVA mixture. The AgNWs were added dropwise while stirring to prevent clumping, and the entire mixture was further sonicated for an additional 4 minutes to ensure uniform distribution of the nanowires throughout the matrix. The final nanocomposite solution was then cast into Petri dishes and allowed to settle. To remove excess solvent and promote film formation, the samples were left to dry at room temperature under ambient conditions for approximately one week. This slow drying process facilitated the formation of uniform, crack-free composite films. The concentrations of the active components were optimized based on preliminary trials and maintained constant throughout the study. Specifically, the GO content was fixed at 3 wt% relative to the mass of PVA, while the concentration of AgNWs was kept at 1 wt%. These concentrations were selected to ensure adequate dispersion and to investigate the synergistic effects of GO and AgNWs within the PVA matrix.

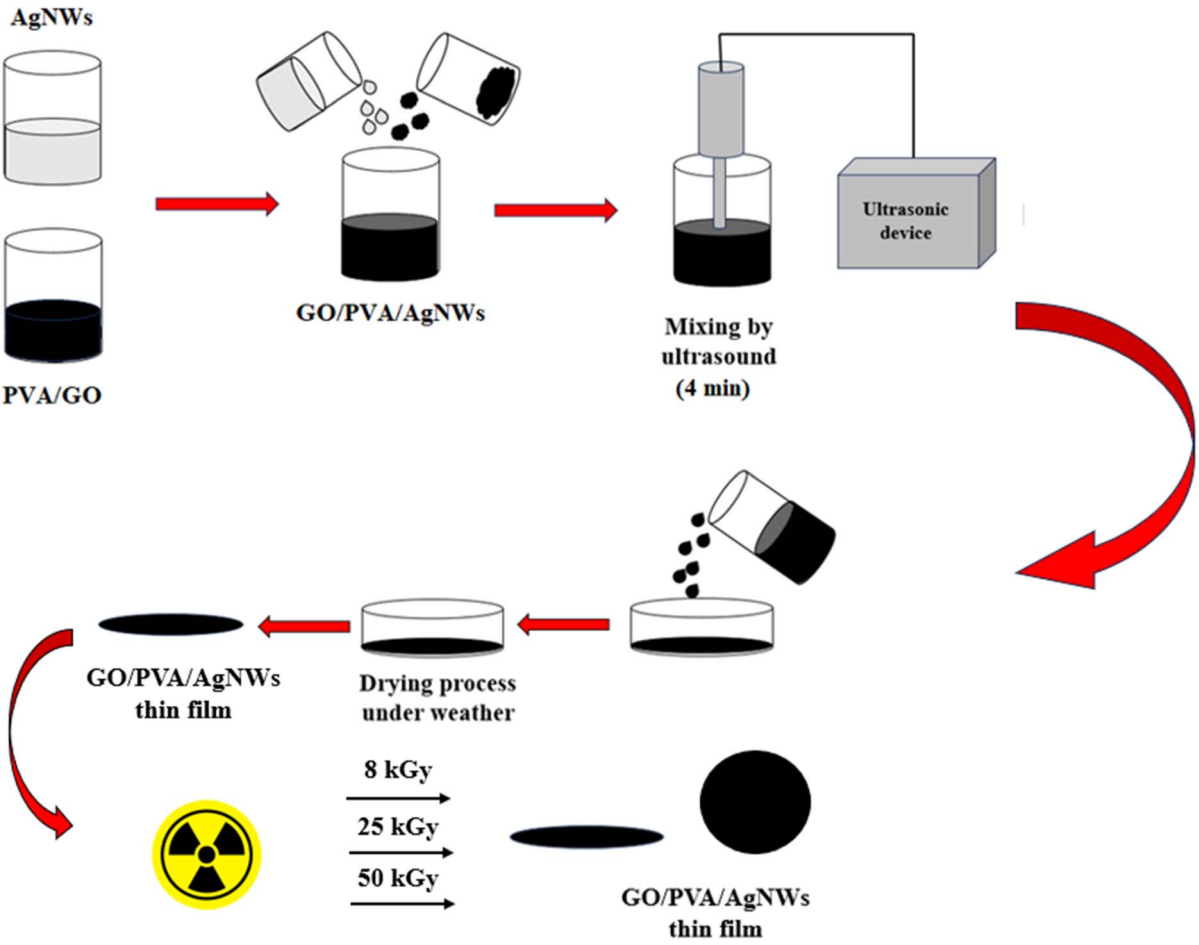

Fig. 1 Preparation of GO/PVA/AgNWs nanocomposites and the effect of gamma radiation.

Upon complete drying, the resulting GO/PVA/AgNWs nanocomposite films were carefully removed and cut into appropriate sizes for subsequent irradiation. The samples were then exposed to gamma radiation at doses of 8, 25, and 50 kGy using a cobalt-60 gamma source. The irradiated samples were subjected to comprehensive structural, morphological, and spectroscopic analyses to evaluate the effects of gamma radiation on the physicochemical properties of the nanocomposites.

2.4 Characterization

The structural properties of the synthesized samples were analyzed using a Rigaku Mini Flex 600 X-ray diffractometer (λ = 1.5406 Å) with Ni-filtered Cu Kα radiation. Low-vacuum SEM backscattered-electron imaging was carried out at 5 kV accelerating voltage and pressure of 50 Pa using Apreo 2S (Thermo Fisher Scientific). Light microscopy in brightfield mode was done using Axio Imager.Z2m. Transmission Electron Microscopy (TEM) was performed with a JEM-1400 (JEOL, Japan) at 80–120 kV.

The vibrational properties of the samples were examined using Raman spectroscopy with a WITec Alpha 300 RS scanning confocal Raman microscope. Raman measurements were conducted in a backscattering geometry, utilizing a frequency-doubled Nd:YAG laser (532 nm) focused through a 100×/0.9 microscope objective. The laser power used during measurements was approximately 1.4 mW. Gamma irradiation experiments were carried out using a ^{60}Co gamma source. The average energy of the γ-radiation was 1.25 MeV, with the gamma quantum energy approximately 1.33 MeV.

3 Results and discussion

3.1 X-ray diffraction analysis

The structural analysis of GO/PVA/AgNWs nanocomposites before and after gamma irradiation is presented in Fig. 2. Fig. 2A corresponds to the non-irradiated sample, while Fig. 2B–2D represent samples irradiated with gamma doses of 8, 25, and 50 kGy, respectively. The broad peak at 2θ = 19.88° is characteristic of PVA (JCPDS 36-1451).[34] Additionally, peaks at 2θ = 38.49°, 45.21°, 64.82°, and 81.78° correspond to the (111), (200), (220), and (311) planes of AgNWs, as indexed in JCPDS card no. 04-0783.[32] Notably, peaks characteristic of GO, located at 2θ = 10.97° and 42° (indexed as (001) and (100), (JCPDS card #75-2078)), were not observed in the XRD diffractogram. This absence suggests that GO was fully dissolved in the PVA matrix and distributed homogeneously throughout the composite.[35]

Fig. 2-1 and 2 illustrate the structural analysis of the top and bottom layers of the GO/PVA/AgNWs nanocomposites,

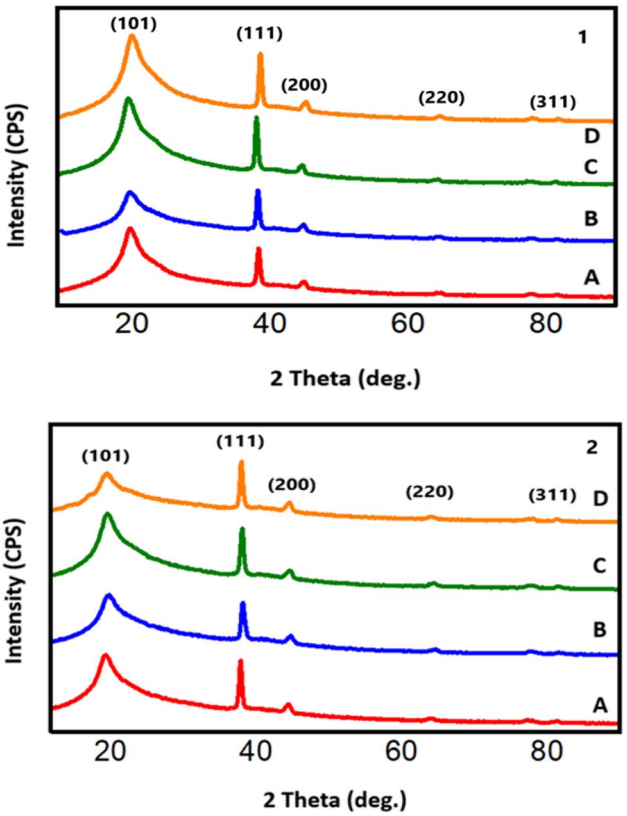

Fig. 2 XRD diffraction patterns of GO/PVA/AgNWs nanocomposites: 1 – top layer, 2 – bottom layer: (A) non-irradiated sample, (B) irradiated at 8 kGy, (C) irradiated at 25 kGy, (D) irradiated at 50 kGy.

respectively. It is important to note that the peak positions are identical for both layers. However, the intensity of the peaks attributed to Ag is higher in the bottom layer (Fig. 2-2). This indicates that the filler preferentially accumulates in the lower regions of the polymer composite, likely due to gravitational forces during the drying process at room temperature.[36] Furthermore, the broader half-width of the XRD peak for PVA in the bottom layer suggests increased filler accumulation, chain scission of the polymer, and a reduction in the degree of polymer crystallinity. In the non-irradiated samples, the half-width of the PVA peak is 3.08°. After ϒ irradiation, the half-width for the bottom layer increased to 3.48°, 3.49°, and 4.03° for doses of 8, 25, and 50 kGy, respectively. In contrast, the top layer showed a more modest increase from 3.08° to 3.36°. This disparity can be attributed to the filler accumulation in the bottom layer acting as a cross-linking center under gamma radiation. This reduces crystallinity, decreases crystallite size, and alters the strain within the crystal structure.

3.2 Morphology

3.2.1 Optical microscopy. Fig. 3 shows the optical microscope images of the GO/PVA/AgNWs composite obtained in reflection mode. Fig. 3A corresponds to the top layer of the composite, where the silver nanowires are observed to be homogeneously distributed. Additionally, the AgNWs exhibit random orientations rather than alignment in a single

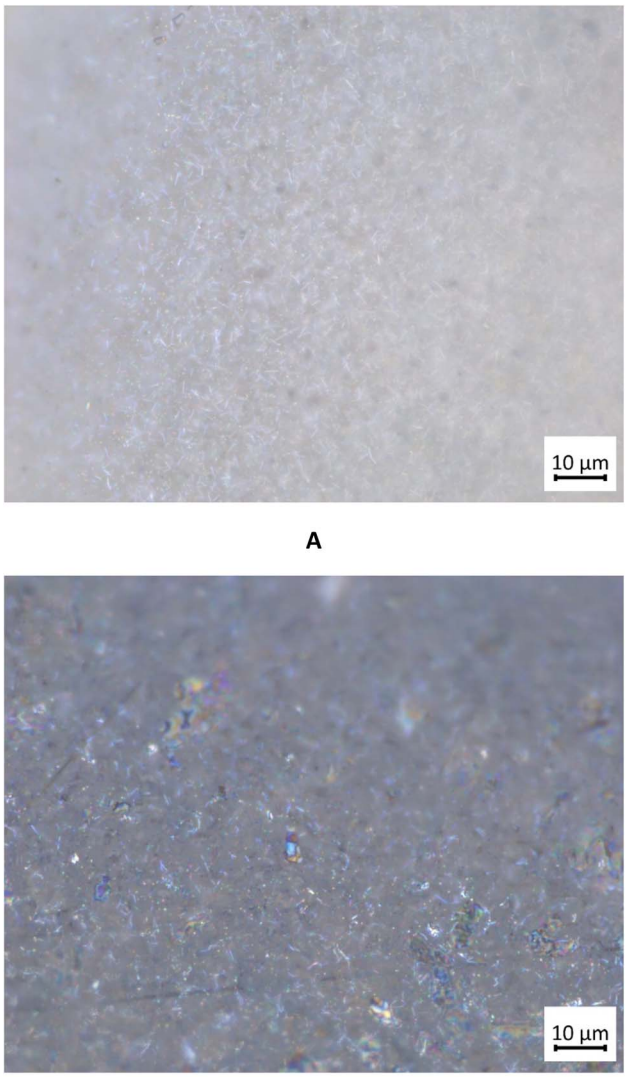

Fig. 3 Optical microscope images of GO/PVA/AgNWs composite: (A) top layer, (B) bottom layer for GO/PVA/AgNWs.

direction. Bright spots in the image represent AgNWs oriented perpendicularly to the surface. Fig. 3B represents the bottom layer of the composite. As seen in the image, this layer appears darker, which is attributed to the greater distribution of GO in the lower regions, reducing the reflectivity. Furthermore, in addition to silver nanowires, bulkier particles are observed in this layer. These particles are likely silver structures that did not form nanowire shapes during synthesis. The absence of such bulky particles in the upper layer can be explained by their higher mass, which causes them to settle in the lower regions of the polymer under the influence of gravitational forces during the drying process.

3.2.2 TEM and SEM analysis. Fig. 4 displays the TEM images of the synthesized GO and AgNWs. Fig. 4A and B correspond to GO samples. As shown, the synthesized GO exhibits a multilayered structure with varying degrees of folding and wrinkling. Not all GO sheets consist of the same number of

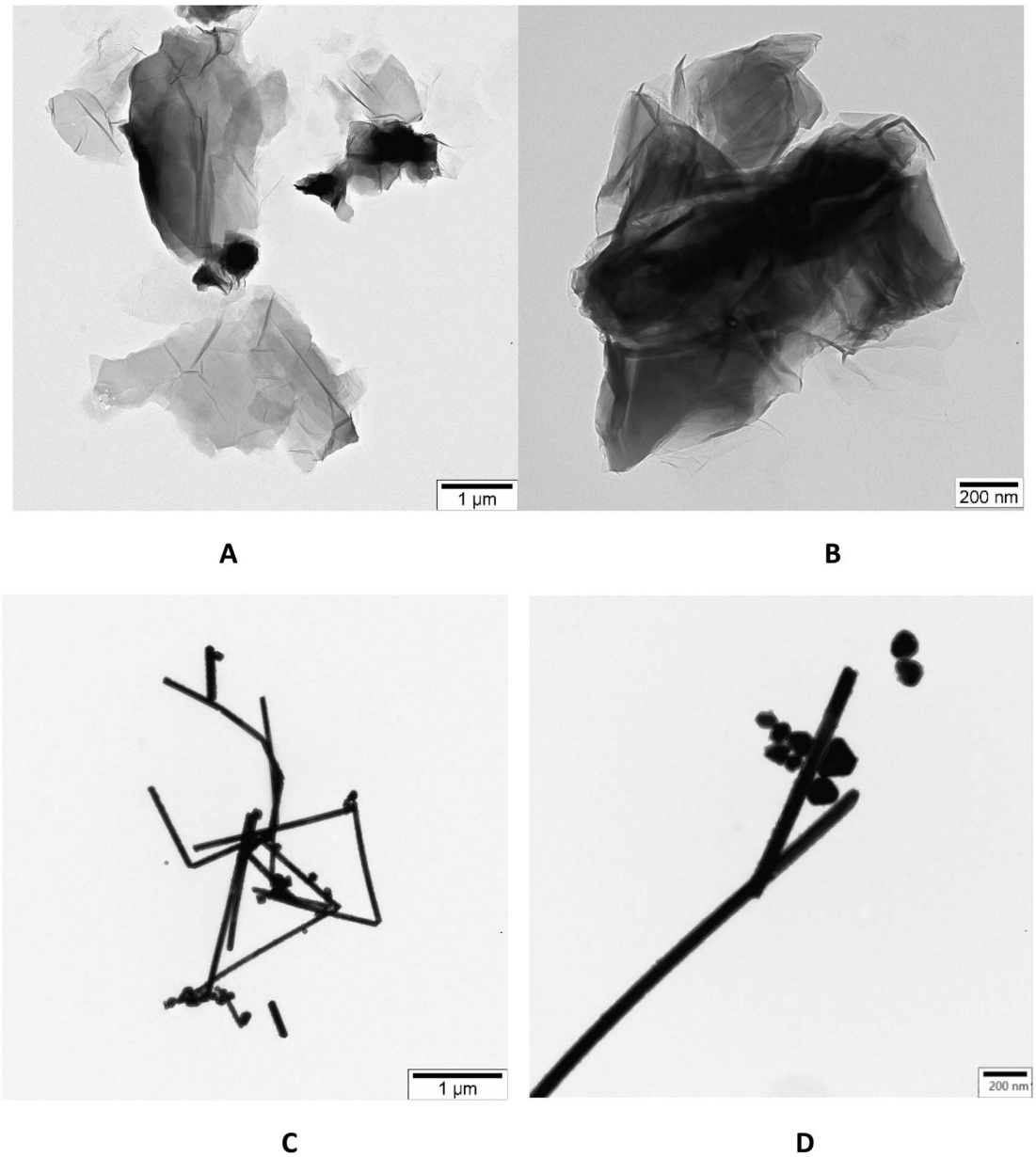

Fig. 4 TEM images of nanomaterials: (A and B) GO nanosheets, (C and D) Ag nanowires.

layers; Fig. 4A highlights instances of single-layer GO sheets. Furthermore, the size of the synthesized GO sheets spans a broad range, with dimensions varying between 0.7 and 2 μm. Fig. 4C and D illustrate the TEM image of AgNWs synthesized *via* the polyol method. The TEM results confirm the successful synthesis of silver nanowires. Based on the TEM analysis, the AgNWs exhibit diameters ranging from 50 to 110 nm and lengths from 2.7 to 5 μm. Additionally, the images reveal the presence of silver particles alongside the nanowires. These particles are attributed to silver structures that did not fully form into nanowires during the synthesis process.

3.2.3 SEM analysis. Fig. 5 illustrates the SEM images of the GO/PVA/AgNWs nanocomposites. Fig. 5A and B correspond to the top surface of the sample. These results confirm the uniform distribution of Ag nanowires in different directions, aligning with the findings from the optical microscope analysis. However, it was also observed that the concentration of silver nanowires varies across the sample. Fig. 5B shows a region with a denser distribution of AgNWs, where randomly oriented nanowires intersect with each other. Fig. 5C and D depict the bottom surface of the GO/PVA/AgNWs nanocomposites. The images reveal bulky silver particles on this surface, which can be attributed to gravitational forces during the formation of the composite.

Fig. 5E displays a cross-sectional SEM image of the sample, revealing a lower concentration of nanoobjects in the upper layer of the composite. The cross-sectional morphology indicates the presence of smaller nanowires predominantly on the

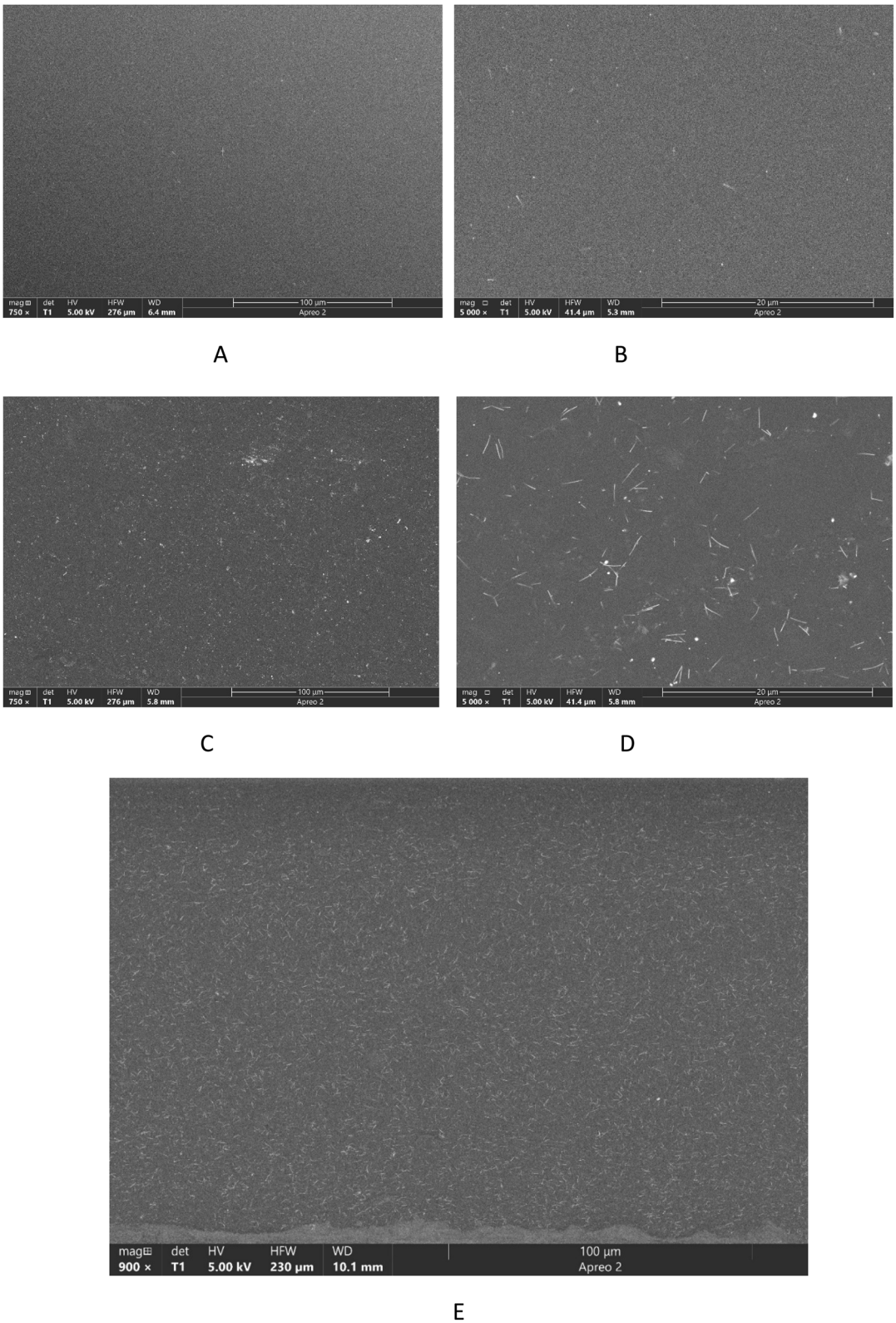

Fig. 5 Typical SEM images of GO/PVA/AgNWs nanocomposites: (A and B) top surface, (C and D) bottom surface and (E) cross-section of the 3% GO/PVA/AgNWs sample.

top side of the sample. This distribution is attributed to gravitational effects and the development of a dense, polymer-rich skin layer at the liquid/vapor interface during solvent evaporation. The composition of this surface layer, whether rich or deficient in nanoparticles, is influenced by the interaction strength between the nanoparticles and the polymer matrix.[37]

It is important to note that ϒ radiation did not induce any noticeable morphological changes in the nanocomposite, as no significant differences were observed between irradiated and non-irradiated samples.

3.3 Raman spectroscopy analysis

The Raman spectra of the GO/PVA/AgNWs nanocomposites reveal two primary bands: D Band (1349 cm^{-1}): this band is associated with the A_1g breathing mode of sp^2 carbon rings, which becomes activated due to structural defects or disorder in the graphene lattice. In graphene oxide (GO), the D band intensity increases as defects introduced by oxidation create sp^3 carbon bonds, signifying the level of disorder or defects in the carbon lattice. G Band (1593 cm^{-1}): This band corresponds to the E_{2g} phonon mode, related to the in-plane vibration of sp^2-hybridized carbon atoms in graphene. The G band represents the graphitic structure, indicating the presence of ordered sp^2 carbon domains within the material. Additional bands were observed at 2677 cm^{-1} and 2912 cm^{-1}. A characteristic band for PVA was identified at 2933 cm^{-1} (Fig. 6).

Upon comparing the spectra depend on irradiation doses (Fig. 6B–D), it can be observed that the positions and presence of peaks are consistent in all cases. However, changes in the intensity ratio of the D and G bands are evident. The ratio of the intensities of the D and G bands (I_D/I_G ratio) is often used to assess the level of disorder or defect density in graphene oxide.[38] A higher I_D/I_G ratio indicates more defects (higher oxidation or more disordered structure), while a lower ratio suggests a more graphitic, ordered structure. The calculated ratios for the samples are presented in Table 1. The sample not exposed to ϒ radiation exhibited the lowest I_D/I_G ratio, indicating the minimal degree of structural disorder. In contrast, samples exposed to ϒ radiation showed higher levels of disorder, with the most significant increase observed in the sample irradiated with an 8 kGy dose. This nonlinear effect of ϒ radiation on structural disorder aligns with previously reported findings.[39]

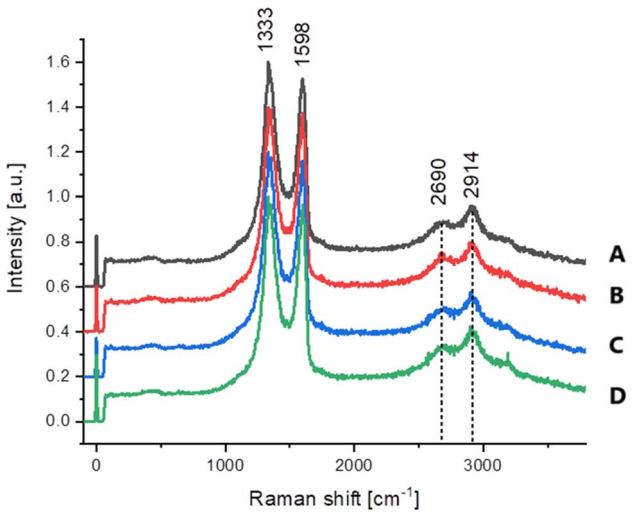

Fig. 6 Raman spectra for GO/PVA/AgNWs nanocomposites: (A) non-irradiated sample, (B) irradiated at 8 kGy, (C) irradiated at 25 kGy, (D) irradiated at 50 kGy.

Table 1 I_D/I_G ratios of GO/PVA/AgNWs nanocomposites irradiated at different doses

GO/PVA/AgNWs	
Dose of gamma irradiation	I_D/I_G
Non-irradiation	1/0.98 = 1.02
8 kGy	1/0.9331 = 1.07
25 kGy	1/0.9628 = 1.04
50 kGy	1/0.9524 = 1.05

4 Conclusion

In this study, GO was synthesized using a modified Hummers' method, while AgNWs were synthesized using a modified Polyol method. Subsequently, GO/PVA/AgNWs nanocomposite materials were prepared using the casting method. The prepared GO/PVA/AgNWs nanocomposites were exposed to ϒ radiation at doses of 8, 25, and 50 kGy for first time. After exposure to ϒ radiation, the structure and morphology of the GO/PVA/AgNWs nanocomposites were investigated, and Raman measurements were conducted. The results indicate that during the preparation of the samples, part of the filler sedimented into the lower layers due to the effect of gravity. Structural analysis shows that the impact of ϒ radiation on the degree of crystallinity was more pronounced on the lower side of the sample due to the sedimentation of nanoparticles. Although the effects of ϒ radiation on morphology were not clearly visible in the morphological analyses, they confirmed the sedimentation of particles under the influence of gravity. Raman results indicate that gamma radiation increased defects and disordered structures in the samples; however, this increase was not linear. The highest disorder was observed in the nanocomposite exposed to 8 kGy, with an I_D/I_G ratio of 1.07.

Data availability

The data that support the findings of this study are available from the corresponding author upon reasonable request.

Conflicts of interest

The authors declare no competing interests.

Acknowledgements

The authors sincerely appreciate the support provided by the European Cooperation in Science and Technology (COST) through the following initiatives: CA19118 – High-performance Carbon-based Composites with Smart Properties for Advanced Sensing Applications (EsSENce) and CA20126 – Network for Research on Porous Semiconductors and Oxides for Innovation and Product Development (NETPORE). Their help in writing the

manuscript, performing measurements, fostering collaborations with international laboratories, and promoting innovation has been crucial and greatly valued.

References

1 S. Verma, S. Mohanty and S. K. Nayak, Preparation of hydrophobic epoxy–polydimethylsiloxane–graphene oxide nanocomposite coatings for antifouling application, *Soft Matter*, 2020, **16**(5), 1211–1226.
2 V. Dhand, G. Mittal, K. Y. Rhee, S. J. Park and D. Hui, A short review on basalt fiber reinforced polymer composites, *Composites, Part B*, 2015, **73**, 166–180.
3 P. Yadav, V. Lahariya, P. P. Pandey, S. Behl and R. Raghav, Investigation of thermal and dielectric behaviour of PVA–ZnO nanocomposite films, *J. Mater. Sci.: Mater. Electron.*, 2023, **34**(9), 787.
4 L. R. Gahramanli, M. B. Muradov, O. O. Balayeva, G. M. Eyvazova and R. M. Mirsultanova, Role of temperature in the growth and formation of CdxZn1-xS/PVA nanocomposites through SILAR method, *Mater. Res. Bull.*, 2021, **137**, 111162.
5 M. Martin, N. Prasad, M. M. Sivalingam, D. Sastikumar and B. Karthikeyan, Optical, phonon properties of ZnO–PVA, ZnO–GO–PVA nanocomposite free standing polymer films for UV sensing, *J. Mater. Sci.: Mater. Electron.*, 2018, **29**, 365–373.
6 S. Shekhar, A. Sarkar, B. Sharma and P. Jain, Electrochemical evaluation of functionalized graphene oxide filled PVA-chitosan biohybrid for supercapacitor applications, *J. Appl. Polym. Sci.*, 2020, **137**(17), 48610.
7 J. Long, A. V. Nand, C. Bunt and A. Seyfoddin, Controlled release of dexamethasone from poly (vinyl alcohol) hydrogel, *Pharm. Dev. Technol.*, 2019, **24**(7), 839–848.
8 W. Xia, H. Xue, J. Wang, T. Wang, L. Song, H. Guo, X. Fan, H. Gong and J. He, Functionlized graphene serving as free radical scavenger and corrosion protection in gamma-irradiated epoxy composites, *Carbon*, 2016, **101**, 315–323.
9 T. N. Ghosh, S. S. Pradhan, S. K. Sarkar and A. K. Bhunia, On the incorporation of the various reduced graphene oxide into poly (vinyl alcohol) nano-compositions: comparative study of the optical, structural properties and magnetodielectric effect, *J. Mater. Sci.: Mater. Electron.*, 2021, **32**, 19157–19178.
10 F. S. Ajizah, A. B. Fitrilawati and N. Syakir, Characteristics of PVA/GO Composite Membranes Prepared Using Solution Casting Technique for Reducing Methylene Blue Concentration, *Jurnal Ilmu dan Inovasi Fisika*, 2023, **7**(1), 20–29.
11 J. Ma, Y. Li, X. Yin, Y. Xu, J. Yue, J. Bao and T. Zhou, Poly (vinyl alcohol)/graphene oxide nanocomposites prepared by in situ polymerization with enhanced mechanical properties and water vapor barrier properties, *RSC Adv.*, 2016, **6**(55), 49448–49458.
12 M. Owais, A. K. Pal, Z. Waris, N. Khoteeva, A. Shiverskii, K. Yusupov and S. G. Abaimov, Enhanced thermal conductivity of reduced graphene oxide reinforced polymer films through a novel GO reduction mechanism, *J. Vinyl Addit. Technol.*, 2024, **30**(6), 1446–1457.
13 I. S. Yahia and M. I. Mohammed, Facile synthesis of graphene oxide/PVA nanocomposites for laser optical limiting: Band gap analysis and dielectric constants, *J. Mater. Sci.: Mater. Electron.*, 2018, **29**(10), 8555–8563.
14 S. Yadav, I. Ibrar, A. Altaee, A. K. Samal, E. Karbassiyazdi, J. Zhou and P. Bartocci, High-Performance mild annealed CNT/GO-PVA composite membrane for brackish water treatment, *Sep. Purif. Technol.*, 2022, **285**, 120361.
15 A. Syuhada, M. S. Shamsudin, S. Daud, G. Krishnan, S. W. Harun and M. S. Aziz, Single-mode modified tapered fiber structure functionalized with GO-PVA composite layer for relative humidity sensing, *Photonic Sens.*, 2021, **11**, 314–324.
16 A. Rose, K. G. Prasad, T. Sakthivel, V. Gunasekaran, T. Maiyalagan and T. J. Vijayakumar, Electrochemical analysis of graphene oxide/polyaniline/polyvinyl alcohol composite nanofibers for supercapacitor applications, *Appl. Surf. Sci.*, 2018, **449**, 551–557.
17 W. Shao, X. Liu, H. Min, G. Dong, Q. Feng and S. Zuo, Preparation, characterization, and antibacterial activity of silver nanoparticle-decorated graphene oxide nanocomposite, *ACS Appl. Mater. Interfaces*, 2015, **7**(12), 6966–6973.
18 N. Pal, S. Banerjee, P. Roy and K. Pal, Cellulose nanocrystals-silver nanoparticles-reduced graphene oxide based hybrid PVA nanocomposites and its antimicrobial properties, *Int. J. Biol. Macromol.*, 2021, **191**, 445–456.
19 M. B. Baghirov, M. Muradov, G. Eyvazova, Y. Azizian-Kalandaragh, S. Mammadyarova, J. Kim, E. Gasımov and F. Rzayev, Effect of sulphidation process on the structure, morphology and optical properties of GO/AgNWs composites, *RSC Adv.*, 2024, **14**(4), 2320–2326.
20 R. M. Attia, N. M. Yousif and M. R. Balboul, Facile synthesis of r GO/Ag/PVA nanocomposites polymeric films by electron beam irradiation for optoelectronic applications, *Opt. Mater.*, 2022, **126**, 112233.
21 A. Ansón-Casaos, J. A. Puértolas, F. J. Pascual, J. Hernández-Ferrer, P. Castell, A. M. Benito, W. K. Maser and M. T. Martínez, The effect of gamma-irradiation on few-layered graphene materials, *Appl. Surf. Sci.*, 2014, **301**, 264–272.
22 M. M. Atta, H. A. Ashry, G. M. Nasr and H. A. Abd El-Rehim, Electrical, thermal and electrochemical properties of γ-ray-reduced graphene oxide, *Int. J. Miner., Metall. Mater.*, 2021, **28**, 1726–1734.
23 L. F. Dumée, C. Feng, L. He, F. M. Allioux, Z. Yi, W. Gao, C. Banos, J. B. Davies and L. Kong, Tuning the grade of graphene: Gamma ray irradiation of free-standing graphene oxide films in gaseous phase, *Appl. Surf. Sci.*, 2014, **322**, 126–135.
24 S. Jain, A. S. Gajarushi, A. Gupta and V. R. Rao, A passive gamma radiation dosimeter using graphene field effect transistor, *IEEE Sens. J.*, 2019, **20**(6), 2938–2944.
25 S. Feizi, A. Mehdizadeh, M. A. Hosseini, S. A. Jafari and P. Ashtari, Reduced graphene oxide/polymethyl

methacrylate (rGO/PMMA) nanocomposite for real time gamma radiation detection, *Nucl. Instrum. Methods Phys. Res., Sect. A*, 2019, **940**, 72–77.

26 Y. Shi, D. Xiong, J. Li and N. Wang, In situ reduction of graphene oxide nanosheets in poly (vinyl alcohol) hydrogel by γ-ray irradiation and its influence on mechanical and tribological properties, *J. Phys. Chem. C*, 2016, **120**(34), 19442–19453.

27 M. Muradov, M. B. Baghirov, G. Eyvazova, L. Gahramanli, S. Mammadyarova, G. Aliyeva, E. Huseynov and M. Abdullayev, Influence of gamma radiation on structure, morphology, and optical properties of GO and GO/PVA nanocomposite, *Radiat. Phys. Chem.*, 2023, **208**, 110926.

28 M. B. Baghirov, M. Muradov, G. Eyvazova, S. Mammadyarova, L. Gahramanli, G. Aliyeva, E. Huseynov and M. Abdullayev, Features of structure and optical properties GO and a GO/PVA composite subjected to gamma irradiation, *RSC Adv.*, 2023, **13**(50), 35648–35658.

29 M. B. Baghirov, M. Muradov, E. Huseynov, G. E. Kochari, R. F. Huseynali and M. Conradi, The influence of gamma radiation on the structure and morphology of AgNWs/GO nanocomposites, *Radiat. Phys. Chem.*, 2025, **226**, 112258.

30 E. H. Sujiono, D. Zabrian, M. Y. Dahlan, B. D. Amin and J. Agus, Graphene oxide based coconut shell waste: synthesis by modified Hummers method and characterization, *Heliyon*, 2020, **6**(8), e04568.

31 X. Chen, Z. Qu, Z. Liu and G. Ren, Mechanism of oxidization of graphite to graphene oxide by the hummers method, *ACS Omega*, 2022, **7**(27), 23503–23510.

32 R. Kandulna and R. B. Choudhary, Concentration-dependent behaviors of ZnO-reinforced PVA–ZnO nanocomposites as electron transport materials for OLED application, *Polym. Bull.*, 2018, **75**, 3089–3107.

33 K. Jhansi, N. Thomas, L. Neelakantan and P. Swaminathan, Controlling the aspect ratio of silver nanowires in the modified polyol process, *Mater. Lett.*, 2023, **344**, 134396.

34 J. Lu, D. Liu and J. Dai, Preparation of highly conductive silver nanowires for electrically conductive adhesives, *J. Mater. Sci.: Mater. Electron.*, 2019, **30**(16), 15786–15794.

35 M. Aslam, M. A. Kalyar and Z. A. Raza, Graphene oxides nanosheets mediation of poly (vinyl alcohol) films in tuning their structural and opto-mechanical attributes, *J. Mater. Sci.: Mater. Electron.*, 2017, **28**, 13401–13413.

36 M. Inaba, Y. Chen, S. Seike, J. Hirotani, M. Nakano and J. Suehiro, Effect of the gravitational force on electrical alignment of diamond filler particles in polydimethylsiloxane-based heat-conduction sheets, *Diamond Relat. Mater.*, 2024, **146**, 111246.

37 S. Cheng and G. S. Grest, Dispersing nanoparticles in a polymer film via solvent evaporation, *ACS Macro Lett.*, 2016, **5**(6), 694–698.

38 P. Tiamduangtawan and K. Saenboonruang, Environmental-friendly synthesis of reduced graphene oxide (rGO) using gamma irradiation, *J. Phys.: Conf. Ser.*, 2019, **1285**(1), 012034.

39 N. Chadha, R. Sharma and P. Saini, A new insight into the structural modulation of graphene oxide upon chemical reduction probed by Raman spectroscopy and X-ray diffraction, *Carbon Lett.*, 2021, **1**, 1–7.